

ANALYSIS OF FREQUENCY CHARACTERISTICS ON NON-INVASIVE ULTRASONIC-DOPPLER FLOW MEASUREMENT FOR METAL PIPES

Masami Kishiro*, Noritomo Hirayama**, Hironobu Yao*, Toshihiro Yamamoto*, Yasushi Takeda***

*Fuji Electric Instruments Co., Ltd. Field Instrument Development Department,
1, Fuji-machi, Hino-city, Tokyo, 191-8502, Japan, E-mail: kishiro-masami@fujielectric.co.jp

**Fuji Electric Advanced Technology Co., Ltd. Electronic Equipment Technology Laboratory,
1, Fuji-machi, Hino-city, Tokyo, 191-8502, Japan

***Div. Mechanical Science Graduate School of Engineering Hokkaido University,
Kita-13, Nishi-8, Sapporo 060-8628, Japan

ABSTRACT

According to the authors' experiments, the accuracy of non-invasive Ultrasonic-Doppler Velocity Profile (UVP) method is influenced by excitation frequency of ultrasonic transducer, especially for metal pipes, depending on their materials, thickness and diameter.

In this paper, it is considered that the frequency characteristics are caused by acoustic dispersion due to Lamb waves. A model for the analysis was made so that L (longitudinal) waves in plastic wedge, which incide obliquely into metal/plastic pipe, would split into L wave, SV (shear vertical) wave, and Lamb waves in different modes with constant frequency secured. Then, the frequency characteristics were calculated based on this multiple-beam model, and it was confirmed that the calculated errors roughly coincide with the measured data.

Lamb waves with angles of refraction near critical angle of 90 degree would cause relatively large errors in case of small diameter pipes. Therefore, as countermeasures, the excitation frequency was set to the average value between two frequencies, where each angle of refraction of Lamb waves reaches the critical angle. It was confirmed that the accuracy is improved approximately within $\pm 1\%$ for metal pipes by taking the countermeasures.

Keywords: UVP, Frequency characteristics, Dispersion, Lamb waves, Critical angle

1. INTRODUCTION

Recently, UVP method has been often reported as a flow mapping technology. Some papers have also shown the performance of UVP flow meter aimed at industrial use, succeeding in highly accurate flow rate measurement mainly as an invasive type flow meter, that is, a flow meter with wetted transducers [1][2].

However, it is the authors' understanding that the study of UVP method as non-invasive flow metering has not been performed in detail so far. The fundamental investigation has been completed at this time on acoustic propagation through metal and plastic pipes in order to develop non-invasive type UVP flow meter. It has been recognized that there are various kinds of acoustic interference waves, of which the influence is remarkable especially for metal pipes.

In this paper, the analysis is described about the frequency characteristics, that is, the accuracy of flow rate measurement is influenced by excitation frequency of ultrasonic transducer. Countermeasures and the effect are also reported so as to improve the accuracy of non-invasive flow measurement by UVP method.

2. PHENOMENA

According to the authors' experiments, the accuracy of non-invasive flow measurement by UVP method is influenced by excitation frequency of ultrasonic transducer.

The effect depends on the material, thickness and diameter, and it is remarkable especially for thin metal and/or small diameter pipes.

Fig-1 shows an example of the frequency characteristics of accuracy, where UVP method was applied to SS (stainless steel) pipe with diameter of 102.2 mm and thickness of 5.9 mm.

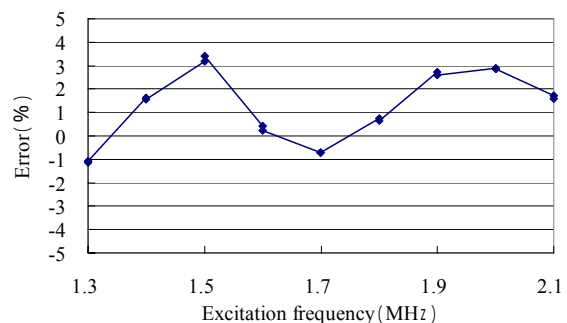


Fig-1: Frequency Characteristics of Accuracy (SS pipe with 102.2 mm dia., 5.9 mm thick)

It is considered that these phenomena are caused by dispersion of ultrasonic waves in metal or plastic pipes, in which sound velocities (i.e. phase velocity, group velocity) change dependently on the excitation frequency.

3. ACOUSTIC DISPERSION

Table-1 shows the kinds of ultrasonic waves that may cause dispersion. There are three kinds. In this table, SH (shear horizontal) waves are irrelevant, because they would not excite L (longitudinal) waves at the interface between pipe and measured liquid. Rayleigh waves are surface waves that attenuate rapidly in the direction normal to the surface. Therefore, it is concluded that only Lamb waves are relevant to the above-mentioned phenomena.

Table -1: List of Acoustic Dispersion

Mode	Kind of wave	Relation to the phenomena
1)SH waves	Shear wave	Irrelevant
2)Lamb waves	Shear + Longitudinal	Relevant
3)Rayleigh waves	Surface wave	Irrelevant

4. LAMB WAVES

Lamb waves are the combination waves of L (longitudinal) waves and SV (shear vertical) waves, and have both natures. Lamb wave is a kind of plate waves, where the plate with finite thickness makes the wave guide, and only specific ultrasounds can propagate through it. Characteristic equations of Lamb waves specify the wavelengths of ultrasounds, satisfying the boundary conditions and depending on the thickness and sound velocities of the plate.

Lamb waves have two modes, symmetric mode and asymmetric mode, as shown in Fig-2. Characteristic equations of Lamb waves are given by Eq. (1):

$$\left. \begin{aligned} \beta_1^2 &= (\omega/V_1)^2 - k^2 \\ \beta_3^2 &= (\omega/V_3)^2 - k^2 \\ \tan(\beta_1 d/2) / \tan(\beta_3 d/2) &= -(k^2 - \beta_3^2)^2 / (4k^2 \beta_1 \beta_3) \\ &\quad \text{(In case of symmetric mode)} \\ \tan(\beta_3 d/2) / \tan(\beta_1 d/2) &= -(k^2 - \beta_3^2)^2 / (4k^2 \beta_1 \beta_3) \\ &\quad \text{(In case of asymmetric mode)} \end{aligned} \right\} \quad (1)$$

where d: thickness, ω : angular frequency, V_1 : sound velocity of L wave, V_3 : sound velocity of SV wave, k: wave number.

Hereafter, each mode of order-number "m" is indicated as S_m and A_m ($m=0,1,2,\dots$) respectively.

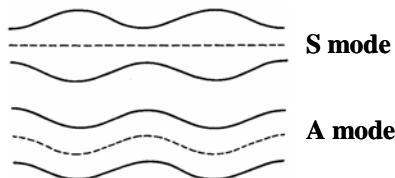


Fig-2: Symmetric Mode and Asymmetric Mode

5. ASSUMPTIONS FOR THE ANALYSIS

For the analysis of the frequency characteristics, the followings are assumed:

1) On phase velocity $V_p = \omega/k$:

Angle of refraction in pipe would be determined by phase velocity in each mode owing to the Snell's law, i.e. $k \sin\theta = \text{const}$.

2) On group velocity $V_g = \partial\omega/\partial k$:

Transit time in pipe would be determined by group velocity of ultrasonic pulse trains, where $V_g \neq V_p$ with dispersion and $V_g = V_p$ without dispersion in general.

3) On acoustic mode conversion at interface:

L wave in plastic wedge, which incides obliquely into pipe, would split into L wave, SV wave and Lamb waves in different modes with constant frequency secured, satisfying the Eq. (1).

The frequency is assumed not to change on the assumption 3), based on the results of the experiment described below.

Fig-3 and Fig-4 show the experimental apparatus for the measurements of waveforms and spectrums of ultrasonic waves penetrated through metal pipe, where the pipe is SS one with diameter of 102.2 mm and thickness of 5.9 mm. The resonance frequency of transducer is 2 MHz. The SS pipe was cut into half, and ultrasonic waves penetrated through it into water were measured by the hydrophone submerged into water. The acoustic absorber made of rubber with tungsten particles was set in front of the ultrasonic transducer for the purpose of absorbing multiple-reflection in SS pipe wall.

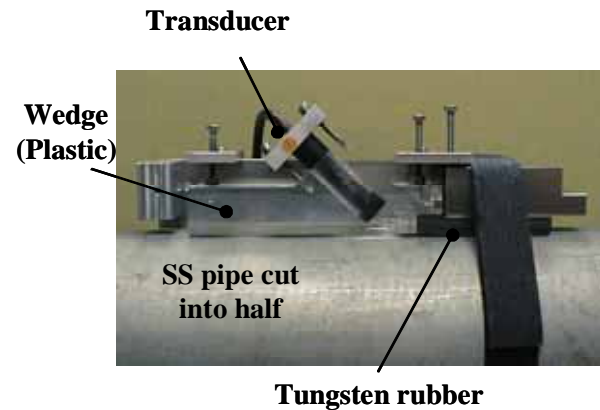


Fig-3: Experimental Apparatus

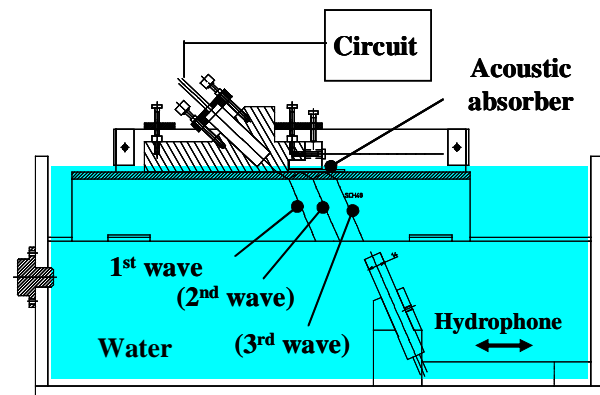


Fig-4: Schematic Diagram of Experimental Apparatus

Fig-5 shows the results of the measurements. The transducer was excited by rectangular 4-pulse waves with basic frequency from 1.5 to 2.0 MHz. The upper waveforms in Fig-5 are ultrasonic waveforms received by the hydrophone,

and the lower curves are their spectrums obtained by FFT function of oscilloscope.

It was experimentally confirmed that central frequencies of spectrums of ultrasonic waves penetrated through SS pipe are roughly equal to the excitation frequencies.

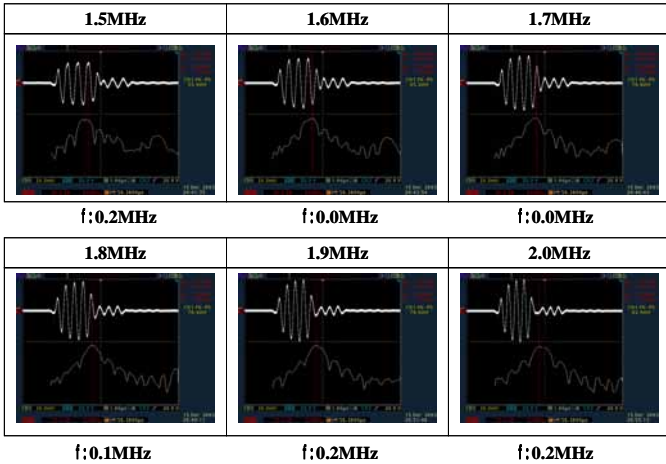


Fig.5: Waveforms and Spectrums of Ultrasonic Waves Penetrated through Metal Pipe (1st wave indicated in Fig-4)

Fig-6 and Fig-7 show the models of split ultrasonic beams at the interface between the plastic wedge and metal/plastic pipe, in accordance with the above-mentioned assumptions 1) to 3). The angles of refraction in pipe θ_p are different from each other owing to the phase velocities of L wave, SV wave, and each mode of Lamb waves.

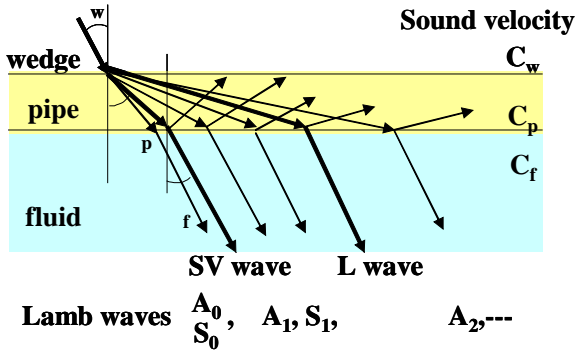


Fig-6: Model of Split Ultrasonic Beams (Case-1: $\theta_w < \theta_c$)

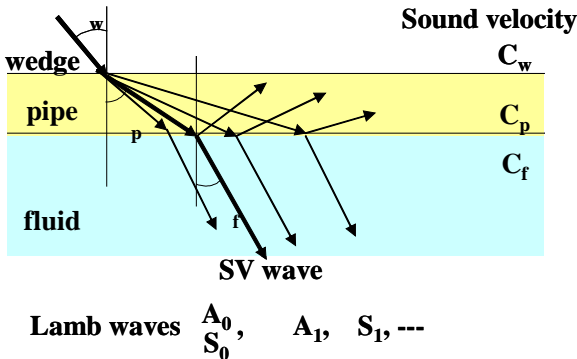


Fig-7: Model of Split Ultrasonic Beams (Case-2: $\theta_w > \theta_c$)

Fig-6 shows Case-1, in which incident angle θ_w is lower than critical angle θ_c for L wave in the pipe, and Fig-7 shows Case-2, in which θ_w is oppositely higher than that so that L wave and higher-ordered Lamb waves are not existent.

The analysis hereafter is performed in Case-2, so that it is simplified.

Fig-8 shows an example of dispersion curves of Lamb waves. On the assumption of constant frequency, the intersection points between the dispersion curves and the horizontal bar corresponding to excitation frequency, show the wave numbers “k” of each mode of Lamb waves. But, all the modes do not necessarily occur, and only such modes occur as having the angle of refraction θ_p of less than 90 degree.

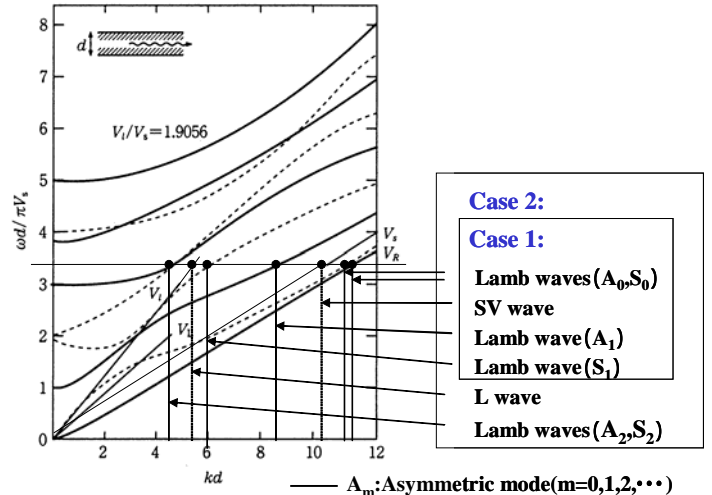


Fig-8: Example of Dispersion Curves of Lamb waves

6. ASYMPTOTIC SOLUTIONS

Phase velocities V_p of Lamb waves are derived from the followings:

$$V_p^{(Am)} = \omega / k^{(Am)}, V_p^{(Sm)} = \omega / k^{(Sm)} \quad (2)$$

In this paper, the superscript (Am) shows asymmetric mode of order number m , and the one (Sm) shows symmetric mode in the same way.

Strictly speaking, $k^{(Am)}$ and $k^{(Sm)}$ in Eq. (2) should be the solutions of Eq. (1).

However, in case that the product of wave number and plate thickness “ kd ” is large, phase velocities V_p of 0-ordered Lamb waves asymptotically come near sound velocity of Rayleigh wave V_R , and V_p of higher-ordered Lamb waves asymptotically come near sound velocity of SV wave V_s .

Asymptotic solutions of phase velocities of Lamb waves V_p are given by the following equations:

- Asymptotic solutions of V_p of 0-ordered Lamb waves:

$$V_p^{(A0)} = V_p^{(S0)} = V_R \quad (3)$$

- Asymptotic solutions of V_p of m -ordered Lamb waves ($m=1, 2, \dots$):

$$\left. \begin{aligned} V_p^{(Am)} &= \omega / \{ (\omega / V_s)^2 - (2m\pi/d)^2 \}^{1/2} \\ V_p^{(Sm)} &= \omega / \{ (\omega / V_s)^2 - ((2m+1)\pi/d)^2 \}^{1/2} \end{aligned} \right\} \quad (4)$$

In the case of analysis in this paper, “ kd ” is nearly 24, where pipe thickness d is 5.9 mm, V_s of SS is 3075 m/s, and transmitted frequency (hereafter excitation frequency is called transmitted frequency) is 2 MHz. Therefore, kd is considered large enough so that the asymptotic solutions of Eq. (3) and (4) are satisfied in following analysis.

Sound velocity of Rayleigh wave V_R is the solution of the following equations:

$$\left. \begin{aligned} L &= \{1 - (V_R/V_1)^2\}^{1/2} \\ S &= \{1 - (V_R/V_s)^2\}^{1/2} \\ 4LS - (1+S^2)^2 &= 0 \end{aligned} \right\} \quad (5)$$

In the case of SS pipe analyzed in this paper, V_R is calculated to 2854 m/s by Eq. (5), where V_1 is 5790 m/s. Therefore, V_R is a little smaller than V_s of above-mentioned 3075 m/s, and has almost no frequency characteristics.

7. FORMULAS FOR THE ANALYSIS

Formulas for the analysis are described below:

$$\left. \begin{aligned} 1) \text{ Angle of refraction: } \theta_p \\ \theta_p^{(Am)} &= \sin^{-1}(V_p^{(Am)}/C_w/\sin\theta_w) \\ \theta_p^{(Sm)} &= \sin^{-1}(V_p^{(Sm)}/C_w/\sin\theta_w) \end{aligned} \right\} \quad (6)$$

where C_w : sound velocity in wedge

$$\left. \begin{aligned} 2) \text{ Group velocity: } V_g \\ V_g^{(A0)} &= V_g^{(S0)} = V_R \\ V_g^{(Am)} &= V_s^2/V_p^{(Am)} \quad (m=1,2,---) \\ V_g^{(Sm)} &= V_s^2/V_p^{(Sm)} \quad (m=1,2,---) \end{aligned} \right\} \quad (7)$$

$$\left. \begin{aligned} 3) \text{ Transit time in pipe: } \tau \\ \tau^{(Am)} &= d/\cos\theta_p^{(Am)}/V_g^{(Am)} \\ \tau^{(Sm)} &= d/\cos\theta_p^{(Sm)}/V_g^{(Sm)} \end{aligned} \right\} \quad (8)$$

$$\left. \begin{aligned} 4) \text{ Radius shift of velocity profile: } r_e \\ r_e^{(Am)} &= C_f (\tau^{(Am)} - \tau^{(Vs)}) \cos\theta_f \\ r_e^{(Sm)} &= C_f (\tau^{(Sm)} - \tau^{(Vs)}) \cos\theta_f \end{aligned} \right\} \quad (9)$$

where C_f : sound velocity in fluid
 θ_f : refraction angle in fluid
 $\tau^{(Vs)}$: transit time of SV wave in pipe

$$\left. \begin{aligned} 5) \text{ Velocity profile of turbulent flow: } V(r) \\ V(r)^{(Am)} &= V_{\max} \{1 - (r - r_e^{(Am)})/R\}^{1/n} \\ V(r)^{(Sm)} &= V_{\max} \{1 - (r - r_e^{(Sm)})/R\}^{1/n} \\ n &= 2.1 \log Re - 1.9 \end{aligned} \right\} \quad (10)$$

where R : radius of pipe
 V_{\max} : maximum velocity of turbulent flow profile
 Re : Reynolds number

8. RESULTS OF THE ANALYSIS

Fig-9 to 12 are the results of the analysis based on the assumptions up to here for the case of Fig-1, where the pipe is SS one with inner diameter of 102.2 mm and thickness of 5.9 mm, and resonance frequency of transducer is 2 M Hz, V_s is 3075 m/s, V_1 is 5790 m/s, incident angle θ_w is 46.9 degree, and sound velocity in wedge is 2730 m/s.

Fig-9 shows the results of calculation of Eq. (6). Refraction angle of mode A_2 of Lamb waves reaches critical angle 90 degree around 1.9 MHz of transmitted frequency, and in the same way that of mode S_1 reaches around 1.4 MHz. These two

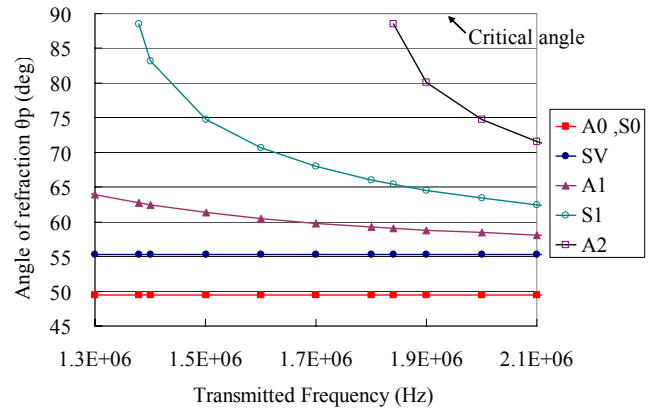


Fig-9: Angle of Refraction vs. Transmitted Frequency (Results of calculation)

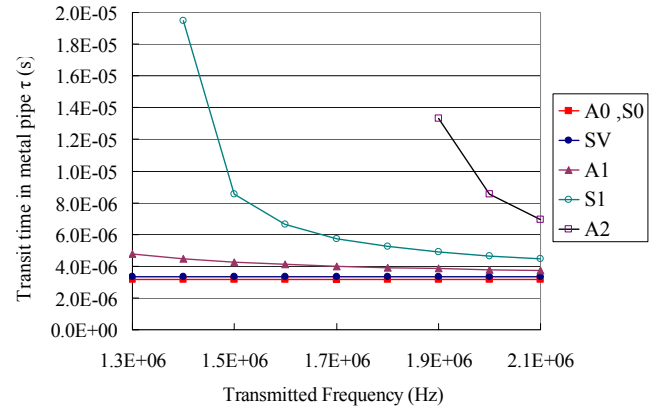


Fig-10: Transit Time vs. Transmitted Frequency (Results of calculation)

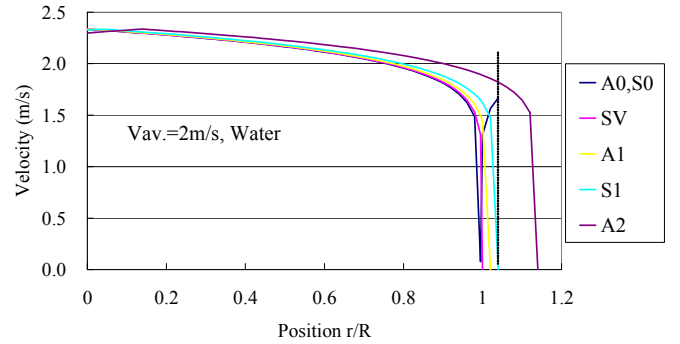


Fig-11: Multiple Velocity Profiles Caused by Differences of Transit Time in SS Pipe (Results of calculation at 2 MHz)

modes are not existent in lower transmitted frequency than them.

Fig-10 shows the results of calculation of transit time by Eq. (8). The SV's straight line shows transit time of SV wave which is originally intended to be used for flow measurement by UVP method. Transit time of the modes A_0 and S_0 of Lamb waves is shorter than that of SV wave, and the transit time of the other higher-ordered modes is longer than that of SV wave. Especially, the modes, whose angles of refraction θ_p are near critical angle 90 degree, have long transit time in the pipe.

Fig-11 shows the results of calculation on the multiple velocity profiles caused by the differences of transit time between SV wave and each mode of Lamb waves, based on Eq. (10), where transmitted frequency is 2 MHz. Each of split

waves has different transit time in SS pipe, because of differences of group velocities V_g and angles of refraction θ_p in SS pipe. It is considered that the original velocity profile got by SV wave and interferential velocity profiles caused by Lamb waves, which shift in horizontal axis owing to different transit time in SS pipe, overlap to each other and induce erroneous velocity profile as a result.

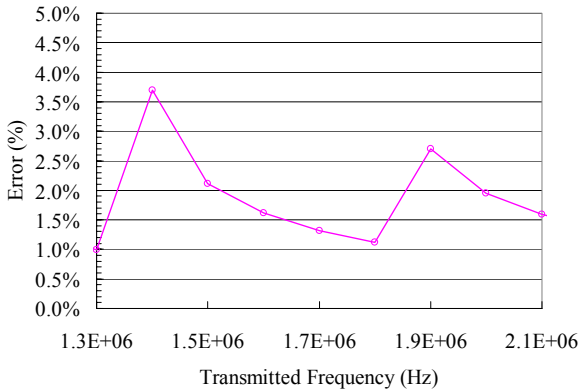


Fig-12: Flow Rate Error vs. Transmitted Frequency (Results of calculation)

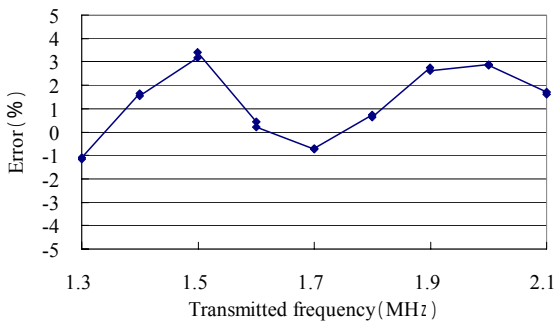


Fig-1: (Re-carried) Flow Rate Error vs. Transmitted Frequency (Results of measurement)

Fig-12 shows the results of calculation on the flow rate error caused by split ultrasounds according to the assumptions up to here. The flow rate error was calculated by averaging multiple profiles and integrating the averaged profile around the central axis of circular pipe section. The flow rate error becomes at the maximum around 1.4 MHz and 1.9 MHz of transmitted frequency, corresponding to the frequencies where angles of refraction for Lamb waves reach critical angle 90 degree in Fig-9.

Compared with the results of Fig-12, the test data of Fig-1 roughly coincides with Fig-12, therefore it is considered that dispersion due to Lamb waves is surely occurring in metal/plastic pipe and induces the frequency characteristics of accuracy for non-invasive UVP flow measurement.

Furthermore, in Fig-12, it must be commented that all split ultrasounds effect on the accuracy equally. In other words, it is assumed that UVP flow meter has the same measuring resolution for all the modes, regardless of their intensity.

As the pipe diameter becomes bigger, the ratio of transit time in pipe to one in liquid becomes smaller. Therefore, the magnitude of frequency characteristics is inversely proportional to the inside diameter of pipe.

Fig-13 shows the test facility used for the measurement of Fig-1. An ultrasonic detector was located by about 10D downstream from a flow conditioner to make the flow axis-symmetric. Air was injected into water from the suction side of upstream pump and broken into micro bubbles as velocity field tracers. Flow rate error was calculated from the average output value in three minutes of UVP flow meter, in comparison with that of an EMF (electromagnetic flow meter) used as the reference meter. The EMF was calibrated within $\pm 0.1\%$ uncertainty. In this paper, all measurements were performed at average velocity of 2 m/s.

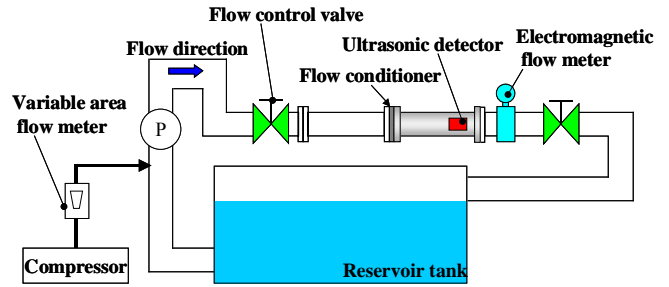


Fig-13: Test Facility of Accuracy Evaluation

9. COUNTERMEASURES AND THE EFFECT

To conquer the frequency characteristics analyzed as above, and to realize high accuracy non-invasive UVP flow meter, countermeasures are taken as below:

1) Specific transmitted frequencies are calculated, where the angles of refraction for all relevant modes of Lamb waves reach critical angle 90 degree. And as shown in Fig-14, the excitation frequency is set to the average value of two of them in the range near resonance frequency of transducer. This is aimed at avoiding the angles of refraction for Lamb waves to become the critical angle, where flow rate error would reach at the maximum.

2) As shown in Fig-14, there is still possibility of occurrence of the offset error even though the excitation frequency is set as described above. Therefore, it is thought that this offset error should be corrected by the actual flow tests, using such standard piping as shown in Fig-13.

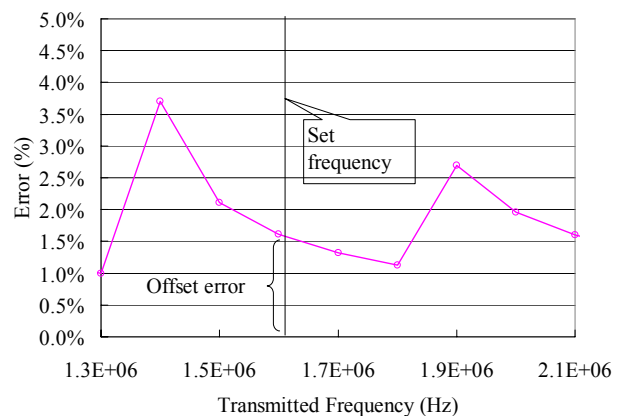


Fig-14: Countermeasures for Frequency Characteristics

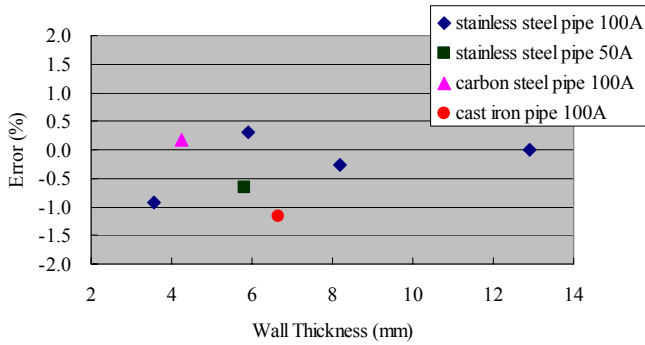


Fig-15: Effect of Countermeasures (2 m/s)

Fig-15 shows the effect of these countermeasures, where pipes are carbon steel, cast iron, and stainless steel with a few kinds of thickness and diameters. The frequencies corresponding to critical angle 90 degree for these pipes were calculated, the excitation frequencies were set to the specific values, and flow rate errors were measured by using the test facility of Fig-13. It was confirmed that the accuracies are approximately within $\pm 1\%$.

10. CONCLUSIONS

In terms of non-invasive UVP flow meter, the frequency characteristics of accuracy for SS pipe approximately coincides with the results of the analysis based on the model of dispersion caused by Lamb waves.

It was confirmed that the accuracy was surely improved by setting the excitation frequency at the average value between two frequencies, where angles of refraction of Lamb waves reach the critical angle.

11. ACKNOWLEDGEMENT

The authors thank to Ph.D. Showko Shiokawa of Shizuoka University in Japan who advised on the analysis in this paper.

12. REFERENCES

1. Y. Takeda, Velocity profile measurement by ultrasound Doppler shift method, *Int. J. Heat & Fluid Flow*, Vol.7, No.4, pp.313-318 (1986)
2. M. Mori, Y. Takeda, T. Taishi, N. Furuichi, M. Aritomi, H. Kikura, 2002, Development of a novel flow metering system using ultrasonic velocity profile measurement, *Exp. Fluids*, 32, pp.153-160.
3. Editorial committee of ultrasonic reference book, 1999, *Ultrasonic reference book*, Maruzen Co., Ltd., pp.62-65.
4. B. A. Auld, *Acoustic Fields and Waves in Solids*, Vol.2, p.80, John Wiley & Sons (1973)
5. K. Negishi, K. Takagi, 1984, *Technology of ultrasonic waves*, University of Tokyo Press, pp.173-174